

# Deformation of Blanketed and Patterned Bilayer Thin-Film Microstructures During Post-Release and Cyclic Thermal Loading

Yanhang Zhang, *Member, ASME*, and Martin L. Dunn, *Member, ASME*

**Abstract**—We study, both experimentally and theoretically, the deformation of blanketed and patterned bilayer thin film microstructures subjected to temperature cycles from room temperature to elevated temperatures following processing by surface micromachining and release from the substrate. While the theoretical treatment is general, the experimental component focuses on beam-like microstructures consisting of a  $0.5\ \mu\text{m}$  thick gold film on a polysilicon film that is either  $1.5\ \mu\text{m}$  or  $3.5\ \mu\text{m}$  thick. For all microstructures the underlying polysilicon film is the same size, but the gold film is patterned into a line that runs the length of the beam. Its width is varied from 0 to 100% of the width of the polysilicon. We experimentally characterize the deformation by measuring the full-field deflection of the gold/polysilicon bilayer beams as a function of temperature using a white-light interferometric microscope. From the deflection, the curvature is determined, and we report the evolution of curvature with the temperature cycling. Qualitatively the behavior is the same regardless of the linewidth. The quantitative differences can be described by a simple model incorporating an inelastic temperature-driven mechanism in addition to linear thermoelastic behavior. We show experimentally and/or analytically, how the parameters in the model vary with linewidth. The results are discussed in the context of the current understanding of microstructural evolution in thin-film metals, and in relation to anticipated thermoelastic response. We show that via a suitable thermal process, the thin film material microstructure can apparently be stabilized over a prescribed temperature range, rendering the subsequent deformation linear thermoelastic. We discuss the implications of these findings in the context of the design and fabrication of high-yield, dimensionally stable MEMS devices utilizing bilayer material systems. Although our measurements are focused on gold/polysilicon bilayer films, the concepts and associated analysis are applicable to other bilayer film systems, particularly ones with metals, although there will surely be quantitative differences. [1007]

**Index Terms**—Bilayers, cyclic thermal loading, inelastic mechanism, linear thermoelastic MEMS.

## I. INTRODUCTION

**M**ULTILAYER material systems play a significant role in many microelectromechanical systems (MEMS) applications. They may serve passive and/or active structural roles. The former include micromirrors where a metal film

is used to yield suitable optical properties. The latter include many microactuators, including bilayers which rely on misfit strains, for example due to thermal expansion mismatch, between two adhering layers. To obtain the necessary thermal expansion mismatch in bilayer actuators, one film is typically a metal and the other a material with a much lower thermal expansion coefficient such as a glass or ceramic. Innovative designs and layering arrangements have led to microactuators capable of deforming both in and out of the plane of the bilayer, providing three-dimensional motion. Such actuators have been used for many purposes including RF switches, optical positioning, accelerometers, and 3-D microassembly [1]–[7]. Irrespective of the intended application, MEMS multilayer material systems are susceptible to substantial deformation upon temperature changes, and their implementation relies on a solid understanding of this behavior, either to use it productively or to compensate for it. In either case, the most straightforward phenomenon to deal with from a design viewpoint is linear thermoelastic behavior where the multilayer deforms linearly with a temperature change. Metal films, however, do not typically exhibit a stable microstructure in their as-deposited state, and exposing them to temperature excursions results in highly nonlinear deformation behavior during the first few cycles due to microstructural evolution such as annihilation of excess vacancies, void coalescence, and grain growth. This phenomenon has been known for some time in the microelectronics materials community [8]–[11] where the primary interest has been in understanding the evolution of stresses in deposited metal lines over a few thermal cycles. It exists in the context of MEMS multilayers, also, and rears its head in the form of short-term and long-term dimensional stability issues due to inelastic deformation mechanisms in the metal. Relevant examples include RF switch arrays [12], tunneling accelerometers [5], and resonant mass sensors [13]. In MEMS applications the film thicknesses are often, but not always, comparable, unlike in microelectronics where the metal film is typically orders of magnitude thinner than the substrate. We refer to the latter as the thin-film limit of the case of two arbitrary thickness films. In the cases where the film thicknesses in MEMS multilayers are not comparable, i.e., one layer is orders of magnitude thinner than the other layer, the studies in microelectronics are directly applicable. Our efforts here are focused on the cases where the film thicknesses are comparable. This leads to quite different stress states in the films because the large stresses that would exist in the thin-film limit are substantially relaxed by bending of the multilayer.

Manuscript received February 14, 2003; revised July 7, 2003. This work was supported by Sandia National Laboratories (Sandia/NSF Lifecycle Engineering Program) and the Air Force Office of Scientific Research (F49620-02-1-0037). Subject Editor E. Obermeier.

The authors are with the Department of Mechanical Engineering, University of Colorado at Boulder, Boulder, CO 80309 USA (e-mail: Martin.Dunn@colorado.edu).

Digital Object Identifier 10.1109/JMEMS.2003.820263

Furthermore, there is a through-thickness stress gradient, unlike in the thin-film limit where the stress through the thickness of the film is essentially constant since the substrate is so thick.

Motivated by microelectronics applications, curvature and stresses have been studied recently for substrates with periodic patterned line geometries [14]–[22]. These studies have focused on both unpassivated and passivated metal lines. Regarding the former, which is most relevant for our purposes, they have shown that patterning in the form of lines can substantially alter the curvature of the film/substrate system and the stress state in the lines both along and across the direction of the lines. In all of these studies the substrate is much thicker than the film and a periodic pattern of lines is considered. As such, these results are not directly applicable to the situation we consider here—a substrate of comparable thickness to the film and a single line on a beam-type structure where the free transverse edges can come into play.

The thermoelastic deformation experienced by such microstructures has been the subject of numerous studies and is fairly well understood, including both linear and geometrically nonlinear deformation [23]. Very little work has focused on inelastic deformation of thin film microstructures subjected to thermal loading [12], [24], [25]. In this work we study the deformation response of thin film bilayer beams during the first few thermal cycles to elevated temperatures (of 100 °C–275 °C) following processing and release from the substrate. While this temperature range is modest compared to similar studies with aluminum and copper films for microelectronics applications, it is quite relevant for practical microsystems applications, including postfabrication packaging processes. Furthermore, it is relevant for optical applications where the optical properties of gold film covered micromirrors have been observed to degrade at temperatures of about 275 °C [26]. Our efforts primarily involve characterization of the deformation response by measuring the full-field deflection of gold/polysilicon bilayer beams as a function of temperature using an interferometric microscope. From the deflection profile we determine the curvature and study its evolution with the temperature cycling. We propose a simple model to describe the observed behavior which incorporates an inelastic temperature-driven mechanism in addition to linear thermoelastic behavior. We discuss the results in the context of the current understanding of microstructural evolution in thin-film metals, and discuss their use for the design and fabrication of reliable devices utilizing multilayer material systems. Regarding the latter, we show that via a suitable thermal process, the microstructure can apparently be stabilized over a prescribed temperature range, rendering the subsequent deformation linear thermoelastic.

## II. SAMPLES AND MEASUREMENTS

We designed a series of gold/polysilicon beam-like microstructures and fabricated them using the MUMPs' surface micromachining process, specifically MUMPs runs 36 and 46 [27]. The process consists of a series of standard microelectronics lithography, thin-film deposition, and etching processes. Briefly, the relevant steps of the complete process consist of depositing a 2- $\mu\text{m}$ -thick sacrificial film of phosphosilicate glass (PSG) on top of a 600-nm-thick silicon nitride film on

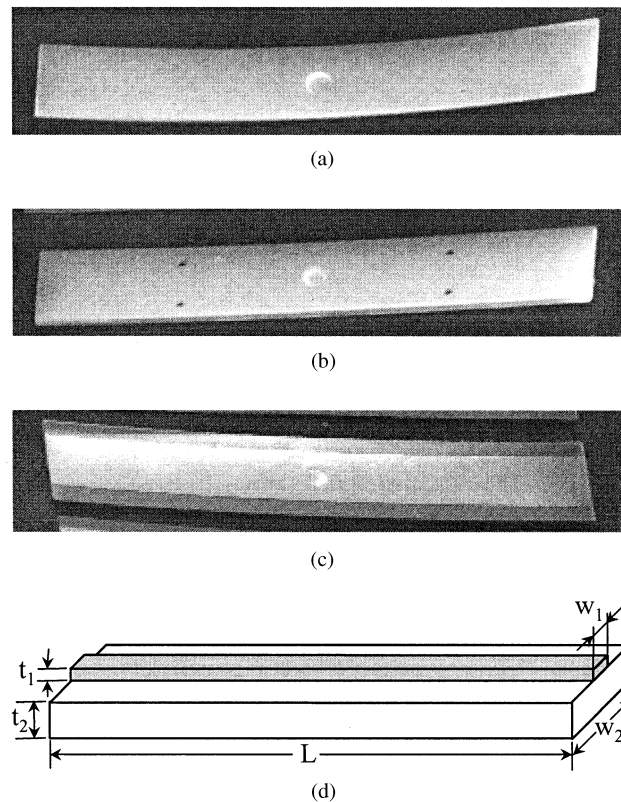


Fig. 1. Scanning electron micrographs (SEMs) of (a) gold (0.5  $\mu\text{m}$  thick)/polysilicon (1.5  $\mu\text{m}$  thick) fully covered; (b) gold (0.5  $\mu\text{m}$  thick)/polysilicon (3.5  $\mu\text{m}$  thick) fully covered; (c) gold (0.5  $\mu\text{m}$  thick)/polysilicon (1.5  $\mu\text{m}$  thick) strip-patterned ( $w_1 = 30 \mu\text{m}$ ) beam microstructures (300  $\mu\text{m} \times 50 \mu\text{m}$ ) supported by a post at the center; and (d) definition of the relevant geometrical parameters.

a (100) single crystal silicon wafer by low pressure chemical vapor deposition (LPCVD). A 2- $\mu\text{m}$ -thick polysilicon film (Poly1) is then deposited on the PSG, patterned, and etched. A 200-nm-thick PSG film is then deposited and the wafer is annealed at 1050 °C for 1 h to dope the polysilicon with phosphorus from both PSG films, and to reduce the residual stress in the polysilicon film. The top PSG and polysilicon films are lithographically patterned and etched to produce the desired beam and plate shapes and sizes. Another 0.75- $\mu\text{m}$ -thick PSG sacrificial film is then deposited, followed by a second 1.5- $\mu\text{m}$ -thick polysilicon film (Poly2), and another 200 nm PSG film to serve as a mask for patterning and etching the Poly 2 layer to conform to the desired beam and plate shapes and sizes. This is followed by another annealing process to minimize residual stresses and stress gradients. A 0.5- $\mu\text{m}$  gold film with a 200- $\text{\AA}$  chromium adhesion layer is deposited, then lift-off patterned [28]. Finally, the polysilicon/gold microstructures are freed from the substrate by etching away the PSG sacrificial film in a 49% hydrofluoric acid solution. In order to assure the etchant attacks the PSG completely and in a timely manner, etch holes are patterned in the microstructures to provide an easy flow path for the etchant. The thin film microstructures are then dried using a supercritical  $\text{CO}_2$  drying process to prevent the beams from sticking to the substrate. Scanning electron micrographs of beam-like microstructures are shown in Fig. 1; the geometrical parameters used subsequently are defined in Fig. 1(d). For each MUMPs' run, Cronos

measures film stresses using wafer curvature. For MUMPs' 46, which is used for all but one measurement, the film stress in the Poly1 and Poly2 films is 12 and 11 MPa, respectively, both in compression. The film stress in the gold is 13 MPa, in tension. Stress gradients in the film result in curvature upon release. For the poly2 beams, the curvature after release is  $-48.7 \text{ m}^{-1}$ ; from this we estimate the stress gradient to be  $7.9 \text{ MPa}/\mu\text{m}$ . For the stacked poly1/poly2 beams, the curvature after release is  $-9.7 \text{ m}^{-1}$ ; from this we estimate the average stress gradient for the beam to be  $6 \text{ MPa}/\mu\text{m}$ .

We use the terminology *beam-like*, recognizing that for the planar aspect ratio ( $L/w_2$ ) of these microstructures, plate theory, rather than beam theory, is formally required to describe the deformation. Nevertheless, for convenience we will refer to the microstructures as *beams*. The length  $L$  of the beams was  $300 \mu\text{m}$  and the width  $w_2$  was  $50 \mu\text{m}$ . Two series of microstructures were fabricated; with polysilicon thicknesses of  $1.5 \mu\text{m}$  (formed from the MUMPs' Poly2 layer) and  $3.5 \mu\text{m}$  (formed from the MUMPs' Poly1 and Poly2 layers). For both series, the gold was evaporated at a nominal thickness of  $0.5 \mu\text{m}$  after deposition of a thin chromium adhesion layer. In addition, beams with patterned gold lines were fabricated with polysilicon thicknesses of  $1.5 \mu\text{m}$  and nondimensional linewidths  $w_1/w_2$  of 0–1.0. The idea behind the design of the microstructures was to yield gold/polysilicon bilayer beam microstructures that were supported as freely as possible. To this end, the beams were supported from the substrate by a  $16 \mu\text{m}$  diameter polysilicon support in the center of the beam.

We measured the deformation of the microstructures as a function of temperature change using an interferometric microscope and a thermal chamber that is covered by a quartz window to allow optical access. The thermal system consists of closed-loop temperature controller, a microscope hot/cold stage, and a cooling system. Full-field measurements of the out-of-plane displacement were made with scanning white light interferometry as the temperature was changed. The resolution of the measured out-of-plane displacements,  $w(x, y)$ , is on the order of a nm as verified by making measurements on standard reference samples; the resolution of the temperature chamber is about  $1 \text{ }^\circ\text{C}$ . A 5X Michelson objective was used yielding a lateral spatial resolution of about  $2.7 \mu\text{m}$ .

The test protocol is designed to carefully study the deformation of the bilayer beams upon release, and then upon subsequent uniform heating and cooling cycles over a temperature range from room temperature to  $100 \text{ }^\circ\text{C}$ – $275 \text{ }^\circ\text{C}$ . This temperature range encompasses the temperature excursions that are expected during many postprocessing and packaging steps. From room temperature, following release, the samples were heated to  $100 \text{ }^\circ\text{C}$  at a rate of about  $200 \text{ }^\circ\text{C}/\text{min}$ . The heating rate varies as the sample temperature approaches the target temperature; within about  $5 \text{ }^\circ\text{C}$  of the target temperature, the heating rate dramatically decreases from about  $200 \text{ }^\circ\text{C}/\text{min}$  to about  $10 \text{ }^\circ\text{C}/\text{min}$  as the temperature slowly approaches the target temperature. When the samples are cooled, the cooling rate is approximately the same as the heating rate for temperatures above about  $50 \text{ }^\circ\text{C}$ . Below  $50 \text{ }^\circ\text{C}$ , the cooling rate decreases to an average cooling rate of about  $50 \text{ }^\circ\text{C}/\text{min}$ . The samples were then heated and subsequently cooled for five more cy-

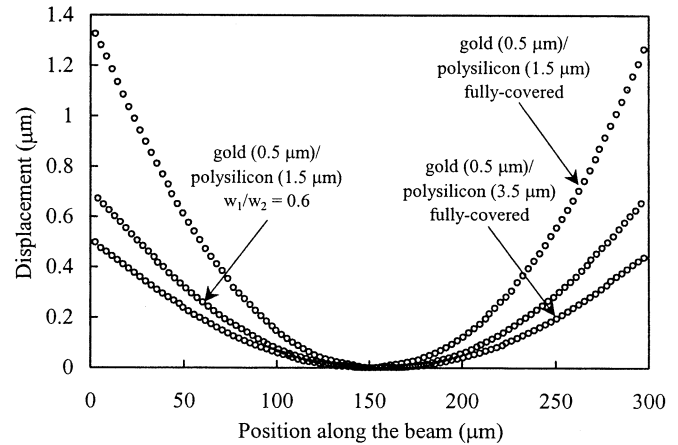


Fig. 2. Measured deflection profiles of the  $L = 300 \mu\text{m}$  beams upon  $\Delta T = -40 \text{ }^\circ\text{C}$ .

cles, with the maximum temperature in each successive cycle increasing by  $20 \text{ }^\circ\text{C}$ . During the heating and cooling cycles, interferograms were obtained at  $20 \text{ }^\circ\text{C}$  increments with the interferometric microscope. At each increment the temperature was held for 3–4 min to make two measurements at thermal equilibrium. Upon temperature changes, the thermal expansion of the MEMS chip and the hot stage produces vertical movement of the microstructures. This can be observed from the motion of the interference fringes on the surface of the microstructures. Thermal equilibrium is typically reached in 3–4 min as indicated by lack of further fringe motion. From the measurements, full-field out-of-plane displacements  $w(x, y)$  of the surface of the beam were determined; typical results are shown in Fig. 2. From the measured displacement field we determined the curvature along the length of the beam (the  $x$ -direction) as  $\kappa(x, y) \approx -\partial^2 w(x, y)/\partial x^2$ . In all cases the curvature was found not to vary with position except within a localized area close to the support post, and thus the deformation is well-described by the average curvature. Although we can not measure them, we are confident that temperature gradients in the temperature chamber contribute insignificantly to the curvature of the gold/polysilicon plate microstructures. This claim is based on measurements of curvature developed in homogeneous single-layer polysilicon beams subjected to the same temperature change: they are about three orders of magnitude less than those developed in the gold/polysilicon beam microstructures.

### III. RESULTS AND DISCUSSION

We begin by discussing the results for the fully covered beams ( $w_1/w_2 = 1$ ). Figs. 3 and 4 show the measurements of curvature versus temperature for the fully covered gold/polysilicon microstructures with both  $1.5 \mu\text{m}$  and  $3.5 \mu\text{m}$  thick polysilicon films. Both microstructures exhibit similar response.

During the initial heating the deformation is thermoelastic, characterized by a decrease in curvature with a constant  $d\kappa/dT$ , until the temperature reaches about  $80 \text{ }^\circ\text{C}$  (the theoretical thermoelastic slope is shown on each figure and is discussed later). Upon continued heating, the curvature changes at a much smaller rate. The small region of pure thermoelastic response (between room temperature and about  $80 \text{ }^\circ\text{C}$ ) is consistent with

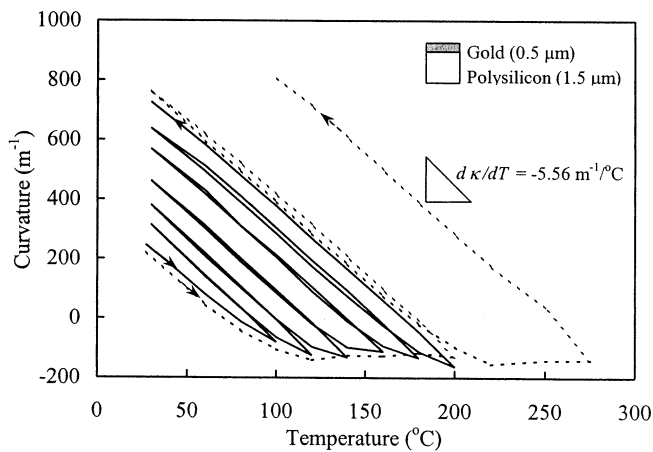


Fig. 3. Curvature versus temperature for gold (0.5  $\mu\text{m}$  thick)/polysilicon (1.5  $\mu\text{m}$  thick)  $300\ \mu\text{m} \times 50\ \mu\text{m}$  beam microstructures. The solid lines are tests with six cycles from room temperature to 200  $^{\circ}\text{C}$  with the maximum temperature in each successive cycle increasing by 20  $^{\circ}\text{C}$ . The dashed lines are tests with two cycles: the first from room temperature to 200  $^{\circ}\text{C}$  and then back to 30  $^{\circ}\text{C}$ , and the second to 275  $^{\circ}\text{C}$  and then back to 30  $^{\circ}\text{C}$ . The arrows indicate the direction at the beginning and end for each set of tests.

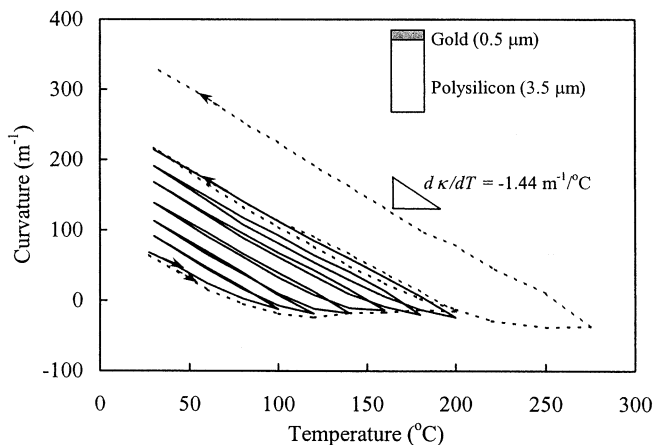


Fig. 4. Curvature versus temperature for gold (0.5  $\mu\text{m}$  thick)/polysilicon (3.5  $\mu\text{m}$  thick)  $300\ \mu\text{m} \times 50\ \mu\text{m}$  beam microstructures. The solid lines are tests with six cycles from room temperature to 200  $^{\circ}\text{C}$  with the maximum temperature in each successive cycle increasing by 20  $^{\circ}\text{C}$ . The dashed lines are tests with two cycles: the first from room temperature to 200  $^{\circ}\text{C}$  and then back to 30  $^{\circ}\text{C}$ , and the second to 275  $^{\circ}\text{C}$  and then back to 30  $^{\circ}\text{C}$ . The arrows indicate the direction at the beginning and end for each set of tests.

results in thin aluminum and copper films on thick silicon substrates, typical of microelectronics applications [8], [11]. The results in [8] and [11], along with results from similar thin film/thick substrate systems, show that  $d\kappa/dT$  often initially exceeds the thermoelastic slope during the first cycle, but that then follows it for some period. This is attributed to plastic relaxation that occurs at room temperature caused by the high film stresses [11].

In our measurements  $d\kappa/dT$  does not initially exceed the thermoelastic slope. This is not necessarily inconsistent with the results of Baker *et al.* [11], though, because the stress levels in our films at room temperature are lower than the yield stress; the polysilicon layer is so thin that the stresses are relaxed by curvature, rather than plasticity (we discuss the stress state in more detail later). Between room temperature and 100  $^{\circ}\text{C}$  the curvature changes from positive to negative, our convention being that

a positive curvature means a beam with the gold on top is curved upward. The existence of a region of  $d\kappa/dT$  that is much smaller than the thermoelastic value is consistent with many findings in thin film/thick substrate systems studied with microelectronics applications in mind (primarily aluminum and copper films on silicon substrates). The behavior in this region apparently results because the microstructure of the evaporated film is not stable in the as-deposited condition. The temperature increase during the first cycle promotes microstructural changes in the film. These result in tensile straining of the film which competes with the thermoelastic deformation [8], [11] resulting in  $d\kappa/dT$  being much smaller than the thermoelastic value. Using high-resolution scanning electron microscopy we have studied the evolution of the gold microstructure during this first cycle. Upon release, the gold microstructure consists of a fine, roughly columnar, grain structure (average grain size about 500 nm). Furthermore, there exists a subgrain structure of about 25–50 nm size. Upon heating to 200  $^{\circ}\text{C}$  and cooling, there appears to be coalescence of the subgrain structure, but no significant growth of the overall grains. This would result in tensile straining of the gold film, consistent with the observed curvature response, although the magnitude of this effect is difficult to quantify. Heating to higher temperatures, say 500  $^{\circ}\text{C}$ –600  $^{\circ}\text{C}$ , and holding for longer times leads to observable grain growth, but associated with this is a loss of reflectivity of the gold so we do not study the behavior at these elevated temperatures. Upon cooling from 100  $^{\circ}\text{C}$ , the response is again thermoelastic, this time throughout the entire cooling process. This is in contrast to similar results for aluminum and copper films for microelectronics where yielding can occur upon cooling [8], [9], [11]. The reason for this difference, though, is because the temperature change in our experiments is much smaller than in most others; for example, the  $\Delta T$  during our first cycle is only about 80  $^{\circ}\text{C}$ , while that during the experiments of Baker *et al.* [11] is about 600  $^{\circ}\text{C}$ . The curvature upon return to room temperature is larger than that initially at room temperature. The  $\kappa - T$  behavior during this first cycle, and during subsequent ones for that matter, is similar in character to the stress-strain response of metals exhibiting plasticity: elastic-plastic behavior during loading, followed by elastic unloading resulting in a permanent plastic strain.

As a point of reference, we have frequently referred to studies of thin film/thick substrate systems motivated by microelectronics. In discussing the second and subsequent cycles in our tests, a direct comparison to results from microelectronics applications is not appropriate. This is because in all microelectronics studies the first cycle is taken to a temperature high enough, and apparently for a time sufficient enough, to stabilize the material microstructure. As a result, the thermomechanical behavior of the second and subsequent cycles is the same. In our tests we have not taken the material to a temperature high enough to fully stabilize the gold microstructure in the first cycle. As a result, subsequent cycles going to successively higher temperatures appear to have the effect of continuing to stabilize the microstructure. In our tests, the response during the second cycle is similar to the first with the exception that the temperature change required to initiate inelastic behavior is increased; again the response is similar to the elastic-plastic response of a metal. Indeed, over the range of temperature cycles studied

in our tests, each subsequent cycle is similar, exhibiting thermoelastic response upon heating until a point where nonlinear  $\kappa - T$  behavior commences. The cooling process is again thermoelastic with the subsequent room temperature curvature increasing with each cycle.

Also shown in Figs. 3 and 4 are results for a second set of tests on nominally identical microstructures with only two cycles: the first from room temperature to 200 °C and back to 30 °C, and the second to 275 °C and back to 30 °C. For both polysilicon thicknesses, the results of the first cycle to 200 °C neatly envelope the results of the set of tests with cycles up to 200 °C. Indeed these results suggest that although there is clearly a path dependence of the deformation behavior, this dependence is controlled by the maximum temperature reached during cycling, independent of how many increments are carried out to reach that temperature. The second cycle to 275 °C shows the same behavior observed in all cycles. For the microstructures with a 1.5  $\mu\text{m}$  polysilicon film, the beam deflection upon cooling from 275 °C becomes too large to measure at about 100 °C. Although we cannot measure it, we expect that the corresponding curvature continues to increase linearly between 100 °C and 30 °C. We also expect that if a cycle were performed at a high enough temperature, the gold film would yield upon cooling resulting in a maximum curvature difference between the as-processed and thermal cycled conditions, consistent with behavior observed in thin film/thick substrate systems. Indeed we have observed these phenomena upon cooling below room temperature, but these results will be presented elsewhere.

The results presented here have been obtained at a constant heating/cooling rate. In terms of the stabilization of the material microstructure which results in inelastic material behavior, the rate, along with the time held at the elevated temperature, will probably play a significant role. Related to this is the behavior during subsequent thermal cycles to a temperature below the maximum reached. For example, if the samples from Figs. 3 and 4 were subsequently thermal cycled to 150 °C, they would be expected to follow the thermoelastic path. Indeed, preliminary data shows this to be the case for hundreds of cycles. Presumably over this range, the microstructure is stable. For cycles in the thousands, though, a gradual shift of the thermoelastic curve downward is observed, possibly due to creep and stress relaxation in the gold, although the thermoelastic slope is maintained [25]. These two issues are obviously closely related and are important, but beyond the scope of this study.

We have repeatedly referred to the response in certain regimes as linearly thermoelastic, meaning the curvature varies linearly with temperature change as predicted by the theory of linear thermoelasticity. In addition, we mentioned the distinction between beams and plates. Now we will take up both of these issues in some detail. Formally, we must treat these microstructures as plates. In fact, for the fully covered beams, the curvature in the transverse direction differs insignificantly from that along the length of the beam. When the displacements are small, the average curvature of a bilayer plate with in-plane dimensions much larger than the thickness,  $\kappa = \kappa_x = \kappa_y$ , depends linearly on the thermal expansion mismatch strain  $\Delta\alpha T$  (where  $\Delta\alpha = \alpha_2 - \alpha_1$ , and  $T$  is the temperature change from a ref-

TABLE I  
PREDICTED AND MEASURED THERMOELASTIC SLOPE  $\eta = d\kappa/dT$  FOR THE FULLY COVERED GOLD/POLYSILICON MICROSTRUCTURES AS A FUNCTION OF THE POLYSILICON THICKNESS

Polysilicon Thickness ( $\mu\text{m}$ )	$\eta$ ( $\text{m}^{-1}/^\circ\text{C}$ )			
	Measured (heating)	Measured (cooling)	Predicted (plate)	Predicted (beam)
1.5	-5.33	-5.38	-5.56	-4.86
3.5	-1.43	-1.41	-1.44	-1.16

erence temperature where  $\kappa = 0$ ) and can be expressed as [29]–[32]

$$\kappa = \frac{6\Delta\alpha T}{t_2} h m \left[ \frac{1+h}{1+2hm(2+3h+2h^2)+h^4m^2} \right] \quad (1)$$

where  $h = t_1/t_2$ ,  $m = M_1/M_2$ , and  $M_i = E_i/1 - \nu_i$  ( $i = 1, 2$ ). In (1) we considered a two-layer plate with layer thickness  $t_1$  and  $t_2$  as shown in Fig. 1(d). Each layer is assumed isotropic and characterized by a Young's modulus  $E_i$ , Poisson's ratio  $\nu_i$ , and thermal expansion coefficient  $\alpha_i$ . In the application to follow, we take layer 1 to be gold and layer 2 to be polysilicon. Equation (1), valid in the regime of small deformations, shows that the bilayer curvature is independent of the plate size and shape. An analysis similar to that which led to (1) can be carried out under the assumption that deformations normal to the long axis of the microstructure are zero, i.e., beam theory. Such an analysis leads to a curvature along the long-axis of the beam given by (1), but with  $\nu_i = 0$  ( $i = 1, 2$ ) and so  $M_i = E_i$ . In the following we apply (1) to model the thermoelastic response of the gold/polysilicon bilayer plates, but do not consider the influence of the thin (20 nm) chromium adhesion layer, since it is so much thinner than the gold and polysilicon films. Calculations show that its contribution to the thermoelastic deformation is negligible. However, the role it plays in the inelastic deformation is unclear due to the lack of complete knowledge regarding the details of the deformation mechanisms.

Figs. 3 and 4 show the linear thermoelastic slope  $\eta = d\kappa/dT$  predicted by (1) as used for plates. It depends on the thermoelastic properties, thicknesses, and geometrical arrangement through the thickness of the films. The predicted thermoelastic slopes for the two microstructures are also shown in Table I, along with the average measured slope during the heating and cooling cycles. Calculation results for both plates and beams are tabulated. In all calculations both the gold and polysilicon are modeled as linear thermoelastic with isotropic material properties. Input parameters are  $E_2 = 163$  GPa,  $\nu_2 = 0.22$  (in line with many measurements over many MUMP's runs; [33]),  $E_1 = 78$  GPa,  $\nu_1 = 0.42$  [34]. The thermal expansion coefficients of the materials are assumed constant and their average values over the temperature range considered are  $\alpha_2 = 2.8 \times 10^{-6}/^\circ\text{C}$ , and  $\alpha_1 = 14.4 \times 10^{-6}/^\circ\text{C}$  [34]. Although some uncertainty exists in the values of these material properties for the gold and polysilicon films, we think that they are accurate enough for the purpose of modeling the observed phenomena. Good agreement exists between the predictions using plate theory and the measurements while predictions based on beam theory are significantly less accurate, demonstrating the need to use plate, rather than beam, theory.

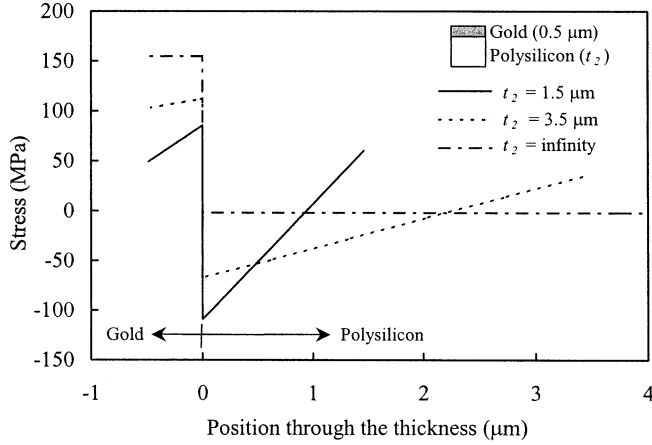


Fig. 5. Stress distributions through the thickness in the gold and polysilicon layers for gold/polysilicon microstructures for a temperature change of  $-100\text{ }^{\circ}\text{C}$ .

While we have focused on the deformation of the gold/polysilicon microstructures, in Fig. 5 we show the corresponding stress distributions through the thickness of the gold and polysilicon layers based on linear plate theory when subjected to a temperature drop of  $100\text{ }^{\circ}\text{C}$ . The stress scales linearly with the temperature change so results for different temperature changes can be obtained by simply scaling the results in Fig. 5. In these calculations based on plate theory the stress is biaxial in the plane of the microstructure, and is uniform. In practice this assumption is accurate except for regions very near the edges and the center support; we verified that this was the case by carrying out full-field finite element calculations. The stress varies linearly through the thickness in both the gold and polysilicon films. For the temperature drop considered here, the stress in the gold layer is in tension; its magnitude is larger at the interface than at the free surface. In the polysilicon, the stress is compressive at the gold/polysilicon interface, decreases in magnitude through the thickness of the polysilicon, and becomes tensile at the polysilicon free surface. As the thickness of the polysilicon substrate increases, the slope of the linear stress distribution in both films decreases. In the thin-film limit (a very thick substrate) the stress is essentially constant through the thickness of each layer. The relaxation of stresses by curvature is also evident in these results. The magnitude of the stress in the gold layer is increased by about 50% as the thickness of the polysilicon layer is increased from  $1.5\text{ }\mu\text{m}$  to  $3.5\text{ }\mu\text{m}$ . It increases another 50 percent as the polysilicon layer becomes infinitely thick. However, Figs. 3 and 4 along with Table I show that for the same temperature change, the magnitude of the curvature developed in the gold ( $0.5\text{ }\mu\text{m}$  thick)/polysilicon ( $1.5\text{ }\mu\text{m}$  thick) microstructure is about four times that developed in the gold ( $0.5\text{ }\mu\text{m}$  thick)/polysilicon ( $3.5\text{ }\mu\text{m}$  thick) microstructure. In practice, either curvature or stresses may be critical design criteria; these results represent the tradeoffs between the two.

Although not shown, the evolution of curvature with temperature cycling for the beams with patterned lines is qualitatively identical to that for the fully-covered beams. In fact, for all of the beams with patterned lines, the temperature at which the inelastic behavior commences is about the same; the average of all samples ( $0.1 \leq c = w_1/w_2 \leq 1$ ) is  $105\text{ }^{\circ}\text{C}$  with a standard

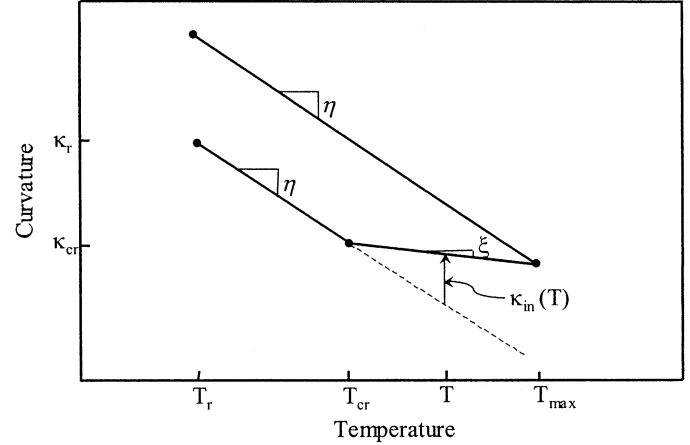


Fig. 6. Schematic diagram showing the parameters in the simple model that describes the curvature versus temperature behavior of the bilayer beam during thermal cycling after release.

deviation of  $2\text{ }^{\circ}\text{C}$ . This suggests that the mechanism responsible for the inelastic behavior is predominately temperature driven. Further evidence leading to this conclusion comes from calculations of the elastic stress state in the gold for a temperature change as a function of  $c = w_1/w_2$ . We have carried out such finite element calculations and found that the average Mises stress in the gold increases by about 60% as  $w_1/w_2$  decreases from 1 to 0.1 for gold ( $0.5\text{ }\mu\text{m}$  thick)/polysilicon ( $1.5\text{ }\mu\text{m}$  thick) bilayer films. This leads us to conclude that the onset of inelastic deformation is driven primarily by temperature, rather than stress. The results in Figs. 3 and 4 along with those for various  $w_1/w_2$  suggest a simple description of the evolution of curvature with temperature as shown in Fig. 6. Four parameters are required: the as-released curvature  $\kappa_r$ , (and the associated release temperature,  $T_r$ ), the critical temperature at which inelastic behavior commences,  $T_{cr}$ , the slope of the  $\kappa - T$  curve in the thermoelastic region,  $\eta$ , and in the inelastic region,  $\xi$ . In general  $\kappa_r$ ,  $\eta$ , and  $\xi$  are functions of the linewidth  $c = w_1/w_2$ , but  $T_{cr}$  is not. The as-released curvature  $\kappa_r$  is determined primarily by the intrinsic stress developed upon film deposition, cooling to room temperature, and release from the substrate. It should be directly related to the film stress that would be measured, for example by wafer curvature, before release. For simplicity we use only the single parameter  $\xi$  to characterize the inelastic response. We could incorporate a more accurate description, say in the form of a power law, but such refinement seems unwarranted presently. With knowledge of  $\kappa_r$ ,  $T_{cr}$ , and  $\xi$ , these three parameters and the thermoelastic slope  $\eta$ , one can readily compute the curvature following a defined thermal loading history. For a thermal cycle from the release temperature  $T_r$  to a maximum temperature  $T_m$ , and back to  $T_r$

$$\begin{aligned}
 \kappa(T) &= \kappa_r + \eta(T - T_r) \text{ for } T_r < T < T_{cr} \quad (\dot{T} > 0) \\
 \kappa(T) &= \kappa_r + \eta(T_{cr} - T_r) + \xi(T - T_{cr}) \text{ for } T_{cr} < T < T_m \quad (\dot{T} > 0) \\
 \kappa(T) &= \kappa_r + \eta(T - T_r) + (\xi - \eta)(T_m - T_{cr}) \text{ for } T < T_m \quad (\dot{T} < 0).
 \end{aligned} \tag{2}$$

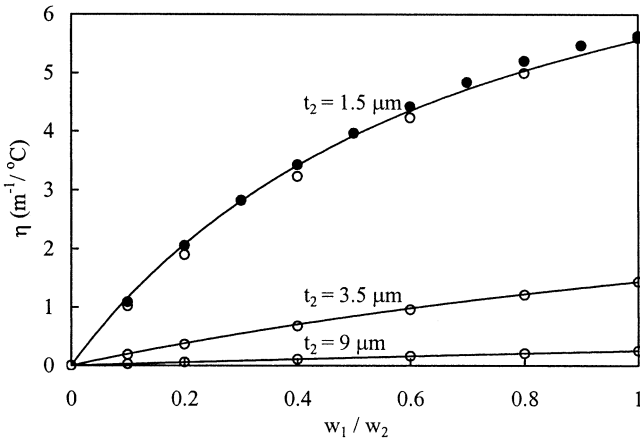


Fig. 7. Thermoelastic slope  $\eta$  versus temperature change as a function of the normalized gold film width for gold ( $0.5 \mu\text{m}$  thick)/polysilicon (thickness =  $t_2$ ) strip-patterned beams. Open circles are finite element simulation results, the solid line is the analytical result of (3), and the filled circles are measurements.

In (2),  $\dot{T} > 0$  denotes heating and  $\dot{T} < 0$  denotes cooling. One can use (2) to describe the curvature evolution after the first and subsequent cycles by simply replacing  $T_{cr}$  with  $T_m$  from the previous cycle and  $(\kappa_r, T_r)$  with the appropriate  $(\kappa, T)$  pair obtained at the end of the previous cycle. In (2),  $T_m$  is then interpreted as the maximum temperature reached in the current cycle.

For our measurements, all microstructures were all released at  $T_r = 25^\circ\text{C}$ , and from the experiments we determined  $T_{cr} = 105^\circ\text{C}$ . Furthermore, it is a reasonable approximation to take  $\xi = 0$ , which simplifies (2) considerably. With these values fixed for all linewidths  $c = w_1/w_2$ , the only parameters that depend on  $c$  are  $\kappa_r$  and  $\eta$ .

With the terms as defined in (1), the curvature of the patterned line structure can be expressed as

$$\kappa_{\text{patterned}} = \frac{6\Delta\alpha T}{t_2} \times hcm \left[ \frac{1+h}{1+2hcm(2+3h+2h^2)+h^4c^2m^2} \right] \quad (3)$$

where  $c = w_1/w_2$  is the nondimensional linewidth; for  $c = 1$ , (3) reduces to (1). In Fig. 7 we plot the variation of  $\eta = \kappa_{\text{patterned}}/T$  with linewidth. The solid lines are predictions from (3) for various thicknesses of polysilicon. Also shown in Fig. 7 are predictions from finite element calculations (open circles) carried out to validate the analytical result of (3), and measurements (filled circles). The finite element calculations and measurements both show that (3) accurately describes the effect of linewidth on curvature development. In practice, many bilayer beams are cantilevered from one end. The tip deflection of a cantilevered beam of length  $L$  that is patterned by a strip described by  $c = w_1/w_2$  can be computed as  $\delta_{\text{tip}} = \kappa_{\text{patterned}}L^2/2$ .

The effect of linewidth on the as-released curvature  $\kappa_r$  is shown in Fig. 8. Previously we argued that  $\kappa_r$  depends primarily on the intrinsic film stresses that result from deposition, but its behavior as a function of linewidth is similar to that of  $\eta$ . This is because although the magnitude of the curvature depends on the intrinsic stresses, the variation with linewidth is related more to

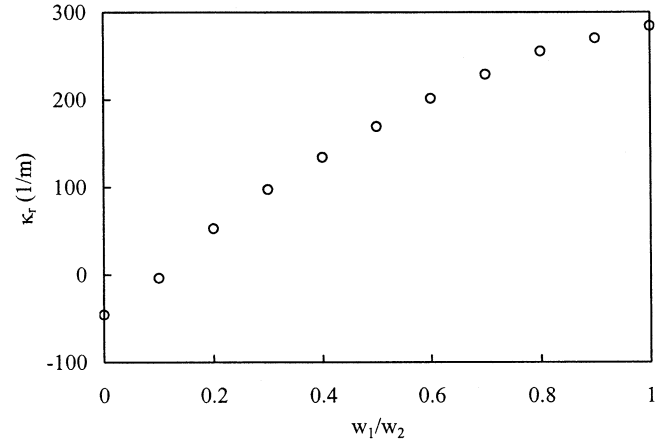


Fig. 8. Curvature after release  $\kappa_r$  as a function of the normalized gold film width for the gold ( $0.5 \mu\text{m}$  thick)/polysilicon ( $1.5 \mu\text{m}$  thick) strip-patterned beams.

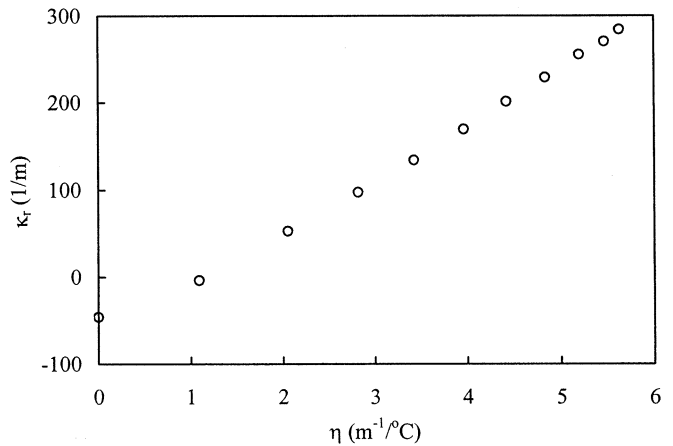


Fig. 9. Curvature after release  $\kappa_r$  vs. thermoelastic slope  $\eta$  for the gold ( $0.5 \mu\text{m}$  thick)/polysilicon ( $1.5 \mu\text{m}$  thick) strip-patterned beams.

the thermoelastic mechanics of the bilayer with internal stresses; these are well described by (3). The release curvature  $\kappa_r$  versus the thermoelastic slope for all  $w_1/w_2$  is also plotted in Fig. 9. The release curvature  $\kappa_r$  increases with  $d\kappa/dT$ , approximately linearly.

We conclude this section by discussing the implications of these results in the design and realization of devices making use of thin film multilayers. As an example, consider a bilayer gold/polysilicon cantilever beam that serves as the active mechanical element in a switch array. During operation there are two key parameters that are strongly impacted by the cyclic thermal behavior discussed above: the linearity of the curvature developed as a function of temperature, and the curvature at room temperature (or any other specified temperature) which sets the reference state for the device. For example in an electrostatically-actuated switch, the room-temperature deflection sets the open or closed configuration, depending on the design, and linear response with a temperature change is desired to facilitate robust temperature compensation schemes. As shown in Figs. 3 and 4, the linearity can be ensured over a certain temperature range by cycling the microstructure to a temperature higher than the maximum intended use temperature, i.e., by an-

nealing it. For example, if the microstructure has been cycled to 200 °C, it can be expected to deform linearly over a temperature range with a maximum temperature less than 200 °C. Again, the complete characterization of the deformation-temperature behavior requires the consideration of the rate of temperature change, and in particular, the length of time the microstructure is held at the elevated temperature [24]. In addition, the thermo-mechanical behavior under cyclic loading can also be important in practice; this has received only limited study, but some aspects have been taken up in [25].

Regarding the room-temperature (or any other temperature) deformation, it can be tailored by a combination of the structural geometry and the annealing process parameters. For the sake of discussion, consider the gold/polysilicon beam microstructure in Fig. 3. Assume that a device application requires that after packaging, the beam is expected to have a curvature of  $300\text{ m}^{-1}$ , for example, to yield a desired tip deflection of a cantilever. In addition, assume that a packaging process, e.g., wire bonding, exposes a microstructure to a temperature of 120 °C. If one simply carried out this process, upon return to room temperature the curvature would be about  $400\text{ m}^{-1}$ , rendering the device unusable. Instead, if an anneal step were performed at 180 °C, for example, the curvature at room temperature after the anneal would be about  $700\text{ m}^{-1}$ . Subjecting it to the 120 °C temperature during the packaging process would induce no further deformation upon return to room temperature since the deformation during that temperature change would be linear thermoelastic. Thus the proper anneal process would make the deformed shape of the microstructure stable during the packaging process. However, the curvature of about  $700\text{ m}^{-1}$ , although stable, would still not be acceptable. The remaining challenge would then be to design the geometry, for example the layout of the gold film on the polysilicon, so that the room-temperature curvature after the anneal was the desired curvature. In the present example this can be accomplished by patterning the polysilicon beam with a gold line—the results shown in Figs. 7–9 can be used to guide the design. This example is intended to demonstrate that if one understands the deformation response, both material and structural, it can be used in the design process to facilitate high device yield. Furthermore, it can be taken advantage of by a clever designer to increase design flexibility.

#### IV. CONCLUSION

We studied the deformation of bilayer beam-like microstructures fabricated by the MUMP's surface micromachining process and subjected to a few temperature cycles from room temperature to elevated temperatures (100 °C–275 °C for the measurements) following processing and release from the substrate. Upon heating the response is linear thermoelastic until a critical temperature is reached and an inelastic deformation, presumably due to microstructural evolution, is activated. The response is again thermoelastic when the beam is cooled to room temperature. Qualitatively this behavior is unchanged if the polysilicon beam is not covered fully by gold but is covered only with a line. We developed a simple model to describe the phenomena, and showed experimentally, and in some cases analytically, how the parameters in the model vary with linewidth. We showed that one can take advantage of the deformation phe-

nomena and via a suitable thermal process, the microstructure can apparently be stabilized over a prescribed temperature range, rendering the deformation linear thermoelastic. We discussed the implications of our findings in the context of the design and fabrication of devices utilizing multilayer material systems, and through an example, illustrated how they can be applied. While the experimental component of our study focuses on gold/polysilicon bilayer films, we expect similar phenomena to arise with other metal films, although there will likely be quantitative differences. This appears to be the case with aluminum and copper films on thick substrates as studied in the context of microelectronics applications.

#### ACKNOWLEDGMENT

The authors benefited greatly from discussions with Professor V. Bright at the University of Colorado and D. Miller of Network Photonics in Boulder, Colorado, and thank Professor K. Gall and Dr. Dudley Finch for help obtaining the SEM images used to study the gold microstructure.

#### REFERENCES

- [1] J. S. Go, Y. H. Cho, B. M. Kwak, and K. Park, "Snapping microswitches with adjustable acceleration threshold," *Sens. Actuators A, Phys.*, vol. 54, pp. 579–583, 1996.
- [2] C. L. Chang and P. Z. Chang, "Innovative micromachined microwave switch with very low insertion loss," *Sens. Actuators A, Phys.*, vol. 79, pp. 71–75, 2000.
- [3] Y. Zhang, Y. Zhang, and R. B. Marcus, "Thermally actuated microprobes for a new wafer probe card," *J. Microelectromech. Syst.*, vol. 8, pp. 43–49, 1999.
- [4] D. C. Miller, W. Zhang, and V. M. Bright, "Micromachined, flip-chip assembled, actuatable contacts for use in high density interconnection in electronics packaging," *Sens. Actuators A, Phys.*, vol. 89, pp. 76–87, 2001b.
- [5] D. J. Vickers-Kirby, R. L. Kubena, F. P. Stratton, R. J. Joyce, D. T. Chang, and J. Kim, "Anelastic creep phenomena in thin film metal plated cantilevers for MEMS," in *Mat. Res. DSoc. Symp.*, vol. 657, 2001, pp. EE2.5.1–EE2.5.6.
- [6] H. Sehr, A. G. R. Evans, A. Brunnschweiler, G. J. Ensell, and T. E. G. Niblock, "Fabrication and test of thermal vertical bimorph actuators for movement in the wafer plane," *J. Micromech. Microeng.*, vol. 11, pp. 306–310, 2001.
- [7] Y. Zhang and M. L. Dunn, "A vertical electrostatic actuator with extended digital range via tailored topology," in *Proc. SPIE's 9th Annual International Symposium on Smart Structures and Materials*, vol. 4700, 2002, pp. 147–156.
- [8] W. D. Nix, "Mechanical properties of thin films," *Metallurg. Trans. A*, vol. 20A, pp. 2217–2245, 1989.
- [9] Y. L. Shen and S. Suresh, "Thermal cycling and stress relaxation response of Si-Al and Si-Al-SiO<sub>2</sub> layered thin films," *Acta Metall. Mater.*, vol. 43, pp. 3915–3926, 1995.
- [10] J. Koike, S. Utsunomiya, Y. Shimoyama, K. Maruyama, and H. Oikawa, "Thermal cycling fatigue and deformation mechanism in aluminum alloy thin films on silicon," *J. Mater. Res.*, vol. 13, pp. 3256–3264, 1998.
- [11] S. P. Baker, A. Kretschmann, and E. Arzt, "Thermomechanical behavior of different texture components in Cu thin films," *Acta Materialia*, vol. 49, pp. 2145–2160, 2001.
- [12] D. C. Miller, M. L. Dunn, and V. M. Bright, "Thermally induced change in deformation of multimorph MEMS structures," *Proc. SPIE—International Society for Optical Engineering*, vol. 4558, pp. 32–44, 2001a.
- [13] F. Shen, P. Lu, S. J. O'Shea, K. H. Lee, and T. Y. Ng, "Thermal effects on coated resonant microcantilevers," *Sens. Actuators, Phys. A*, vol. 95, pp. 17–23, 2001.
- [14] I. S. Yeo, P. S. Ho, and S. G. H. Anderson, "Characterization of thermal stresses in Al(Cu) fine lines. I. unpassivated line structures," *J. Appl. Phys.*, vol. 78, pp. 945–952, 1995a.
- [15] —, "Characterization of thermal stresses in Al(Cu) fine lines. II. Passivated line structures," *J. Appl. Phys.*, vol. 78, pp. 953–961, 1995b.

- [16] T. S. Park and S. Suresh, "Effects of line and passivation geometry on curvature evolution during processing and thermal cycling in copper interconnect lines," *Acta Mater.*, vol. 48, pp. 3169–3175, 2000.
- [17] A. Gouldstone, Y. L. Shen, S. Suresh, and C. V. Thompson, "Evolution of stresses in passivated and unpassivated metal interconnects," *J. Mater. Res.*, vol. 13, pp. 1956–1966, 1998.
- [18] A. Widstrom, P. Gudmundson, and S. Suresh, "Thermoelastic analysis of periodic thin lines deposited on a substrate," *J. Mechan. Phys. Solids*, vol. 47, pp. 1113–1130, 1999a.
- [19] —, "Analysis of average thermal stresses in passivated metal interconnects," *J. Appl. Phys.*, vol. 86, pp. 6088–6095, 1999b.
- [20] A. Wikstrom and P. Gudmundson, "Stresses in passivated lines from curvature measurements," *Acta Mater.*, vol. 48, pp. 2429–2434, 2000.
- [21] Y. L. Shen, S. Suresh, and I. A. Blech, "Stresses, curvatures, and shape changes arising from patterned lines on silicon wafers," *J. Appl. Phys.*, vol. 80, pp. 1388–1398, 1996.
- [22] R. M. Keller, S. P. Baker, and E. Arzt, "Stress-Temperature behavior of unpassivated thin copper films," *Acta Mater.*, vol. 47, pp. 415–426, 1999.
- [23] M. L. Dunn, Y. Zhang, and V. Bright, "Deformation and structural stability of layered plate microstructures subjected to thermal loading," *J. Microelectromech. Syst.*, vol. 11, pp. 372–384, 2002.
- [24] Y. Zhang and M. L. Dunn, "Stress relaxation of gold/polysilicon layered MEMS microstructures subjected to thermal loading," in *Proc. MEMS Symp., ASME International Mechanical Engineering Congress and Exposition*, vol. 3, 2001, pp. 149–156.
- [25] K. Gall, M. L. Dunn, Y. Zhang, and B. Corff, "Thermal cycling response of layered gold/polysilicon MEMS structures," *Mech. Mater.*, vol. 36, pp. 45–55, 2004.
- [26] D. M. Burns and V. M. Bright, "Optical power induced damage to microelectromechanical mirrors," *Sens. Actuators A, Phys.*, vol. 70, pp. 6–14, 1998.
- [27] D. A. Koester, R. Mahadevan, B. Hardy, and K. W. Markus. (2001) MUMPs™ Design Rules. Cronos Integrated Microsystems A JDS Uniphase Company. [Online]. Available: <http://www.memsrus.com/cronos/svcsrules.html>
- [28] W. D. Cowan, V. M. Bright, A. A. Elvin, and D. A. Koester, "Modeling of stress-induced curvature in surface-micromachined devices," *Proc. SPIE*, vol. 3225, pp. 56–67, 1997.
- [29] M. Finot and S. Suresh, "Small and large deformation of thick and thin film multilayers: Effects of layer geometry, plasticity and compositional gradients," *J. Mech. Phys. Solids*, vol. 44, pp. 683–721, 1996.
- [30] M. Finot, I. A. Blech, S. Suresh, and H. Fujimoto, "Large deformation and geometric instability of substrates with thin film deposits," *J. Appl. Phys.*, vol. 81, pp. 3457–3464, 1997.
- [31] L. B. Freund, J. A. Floro, and E. Chason, "Extension of the stoney formula for substrate curvature to configurations with thin substrate or large deformations," *Appl. Phys. Lett.*, vol. 74, pp. 1987–1989, 1999.
- [32] L. B. Freund, "Substrate curvature due to thin film mismatch strain in the nonlinear deformation range," *J. Mech. Phys. Solids*, vol. 48, pp. 1159–1174, 2000.
- [33] W. N. Sharpe, "Mechanical properties of MEMS materials," in *MEMS Handbook*, M. Gad-el-Hak, Ed. Boca Raton, FL: CRC, 2001.
- [34] J. A. King, *Materials Handbook for Hybrid Microelectronics*. Los Angeles, CA: Teledyne Microelectronics, 1988.

**Yanhong Zhang** received the Bachelor of Science in engineering mechanics from Tsinghua University, China, in 1998. She received the Masters of Science in mechanical engineering from the University of Colorado at Boulder in May 2000. She is currently working toward the Ph.D. degree in mechanical engineering at University of Colorado at Boulder.

Her research interests are in the design, modeling and test of the thermomechanical behavior of thin film microstructures for microelectromechanical systems (MEMS) applications.

Ms. Zhang is a Member of the American Society of Mechanical Engineers (ASME).



**Martin L. Dunn** received the Ph.D. degree in mechanical engineering in 1992 from the University of Washington, Seattle.

Currently, he is a Professor of Mechanical Engineering, University of Colorado at Boulder. His research interests include the micromechanical behavior (deformation and fracture) of materials and structures for MEMS applications, the micromechanics, and physics of heterogeneous media, including defects, polycrystals, and composites, and the acoustic characterization of material microstructure. He has published over 80 articles in refereed journals on these subjects and has served as the principal or co-principal investigator in grants and contracts in these areas from NSF, AFOSR, NIST, DOE, DARPA, Sandia National Laboratories, and various companies.

Dr. Dunn is a Member of the American Society of Mechanical Engineers (ASME).